aerospace

MDPI

Article

An Energy Efficiency Optimization Method for Electric Propulsion Units during Electric Seaplanes' Take-Off Phase

Shuli Wang [1,2,3], Ziang Li [1] and Qingxin Zhang [2,3,*]

[1] College of Artificial Intelligence, Shenyang Aerospace University, Shenyang 110136, China; wangshuli@sau.edu.cn (S.W.); ziang_li@163.com (Z.L.)
[2] Key Laboratory of General Aviation, Shenyang Aerospace University, Shenyang 110136, China
[3] Liaoning General Aviation Academy, Shenyang 110136, China
* Correspondence: zhangqx2002@163.com

Abstract: The electric seaplane, designed for take-off and landing directly on water, incorporates additional structures such as floats to meet operational requirements. Consequently, during the take-off taxiing phase, it encounters significantly higher aerodynamic and hydrodynamic resistance than other aircraft. This increases energy demand for the electric seaplane during the take-off phase. A mathematical model for energy consumption during this stage was developed by analyzing resistance, using the propeller pitch angle as an optimization variable. This study proposes a coupled energy efficiency optimization method for the take-off phase of an electric seaplane's electric propulsion unit (EPU). The method aims to determine an optimal propeller pitch angle configuration aligned with the seaplane's design criteria. This ensures that the propeller output thrust meets minimal requirements during take-off while enhancing energy efficiency. Experimental validation with the two-seater electric seaplane prototype RX1E-S has demonstrated that selecting the optimal propeller pitch angle can effectively reduce energy consumption by approximately 10.4%, thereby significantly enhancing flight efficiency.

Keywords: electric seaplane; EPU; energy efficiency optimization; prototype test; coupled optimization

Citation: Wang, S.; Li, Z.; Zhang, Q. An Energy Efficiency Optimization Method for Electric Propulsion Units during Electric Seaplanes' Take-Off Phase. *Aerospace* **2024**, *11*, 158. https://doi.org/10.3390/aerospace11020158

Academic Editor: Jae Hyun Park

Received: 8 December 2023
Revised: 6 February 2024
Accepted: 9 February 2024
Published: 15 February 2024

1. Introduction

At present, the issue of energy resources has become increasingly prominent due to severe economic and environmental pollution concerns. Consequently, a growing focus is on new energy sources and power systems [1,2]. Electric aircraft have gained substantial attention due to their high efficiency, environmental friendliness, low noise emissions, and relatively affordable energy acquisition [3], resulting in significant advancements [4]. The aviation industry is advancing towards electrification, aiming to reduce greenhouse gas emissions and noise pollution in aviation, while also lowering operational costs, in alignment with the trends towards environmental sustainability goals [5–7]. Electric aircraft represent the future of aviation development and serve as the primary direction for green aviation [8]. Seaplanes have garnered substantial attention within the domain of electric aircraft [9], considered a vital branch with immense potential [10]. Seaplanes are crucial in enhancing urban connectivity, especially for countries such as China and the United Kingdom, which possess extensive water bodies and face significant land transportation challenges [11,12].

The unique operational environment and intricate power requirements of electric seaplanes underscore the critical role played by the performance and efficiency of the EPU [13,14]. However, the current EPU for electric seaplanes still has several issues, such as a low power-to-weight ratio and lower energy density [15]. Particularly during take-off, an electric seaplane must overcome water surface resistance and generate sufficient thrust to lift off the water. Studies have shown that an electric seaplane consumes approximately 30% of its total energy requirement during the take-off phase in a single-flight mission [13].

Consequently, optimizing the energy efficiency of the EPU during take-off emerges as a pivotal factor in enhancing electric seaplanes' overall performance and sustainability [16].

During take-off, an electric seaplane encounters resistance from both water and air, impeding its forward movement. The resistance an electric seaplane faces refers to the force opposing the direction of its take-off. Its magnitude directly impacts the acceleration performance of the electric seaplane and influences the distance and time required for the take-off taxiing phase [17].

Many scholars have conducted comprehensive and in-depth research on the design and optimization of electric aircraft. In these studies, aspects such as electric motor selection, propeller design, control strategies, energy management, and system integration have received widespread attention. Patrick Wheeler has provided an overview of electric/hybrid propulsion systems, emphasizing the significance of electric motors [18]. Esteban et al. reviewed power management strategies for electric aircraft propulsion systems [19]. Xia Jiyu and colleagues proposed an aerodynamic propulsion coupled model suitable for vectored electric propulsion systems. By integrating theoretical models with empirical engineering models, they achieved real-time and rapid assessment of the aerodynamic and propulsion performance of vectored electric propulsion systems. This approach further facilitates the optimization of the electric propulsion system [20]. Wei Baoze et al. introduced an optimal power control law, enabling automatic propeller pitch and speed adjustment in a variable-pitch EPU based on flight conditions and thrust requirements. This adjustment results in a combination of propeller pitch angles and speeds that minimize power consumption while meeting thrust demands. Experimental verification revealed an approximate 6.3% reduction in energy consumption compared to constant-speed control laws for completing the same flight profile [21]. Shi Zhifu et al. proposed an overall aircraft design optimization method that combines particle swarm algorithms with Etzkorn iterative numerical algorithms. Building upon a numerical model, they identified design parameters as decision variables in scheme design, transforming design goals into optimization objectives and constraints. This method optimizes the overall aircraft design by establishing a multi-constraint model with penalty factors [22]. Konstantinos et al. mentioned the performance optimization of a hybrid propulsion system, emphasizing modeling and power management frameworks evaluated based on single-flight scenarios, aiming to maximize the utilization of new power system prototypes [23]. Giuseppe Palaia and Karim Abu Salem primarily evaluated the mission performance of aircraft equipped with hybrid propulsion systems, providing insights into power strategies for reducing fuel consumption or extending flight range [24]. Amine Benmoussa and his colleagues developed a simulation model capable of estimating flight performance and analyzing aircraft equipped with hybrid electric power units (HEPUs). They examined the impact of various parameters on aircraft performance [25]. Huqi et al. established a three-dimensional numerical wave tank and validated the accuracy of numerical wave generation using linear wave theory. Subsequently, numerical calculations were conducted for seaplanes under different wave heights at the same wavelength. The numerical simulation results showed good agreement with the model experiment outcomes, providing a foundation for further numerical calculations in the optimization of seaplanes [26]. These studies provide substantial guidance for a deeper understanding and enhancement of energy efficiency in EPU.

However, current research on electric aircraft primarily focuses on hybrid/fuel-powered aircraft and land-based planes, with fewer studies dedicated to electric seaplanes. Due to significant differences between seaplanes and land-based aircraft during the take-off taxiing phase, despite extensive scholarly investigations into energy efficiency optimization for land-based aircraft, these findings cannot be directly applied to the take-off phase of electric seaplanes. Therefore, further research and exploration are imperative to address the energy efficiency optimization challenges specific to the take-off phase of electric seaplanes.

The electric seaplane exhibits several characteristics distinct from land-based electric aircraft during the take-off taxiing phase. Based on its hydrodynamic and aerodynamic properties, the entire take-off taxiing process can be segmented into four stages: taxiing,

transitional taxiing, high-speed taxiing, and floating off water [13]. The variations in hydrodynamic and aerodynamic resistance encountered by the electric seaplane within these four stages are depicted in Figure 1 [13].

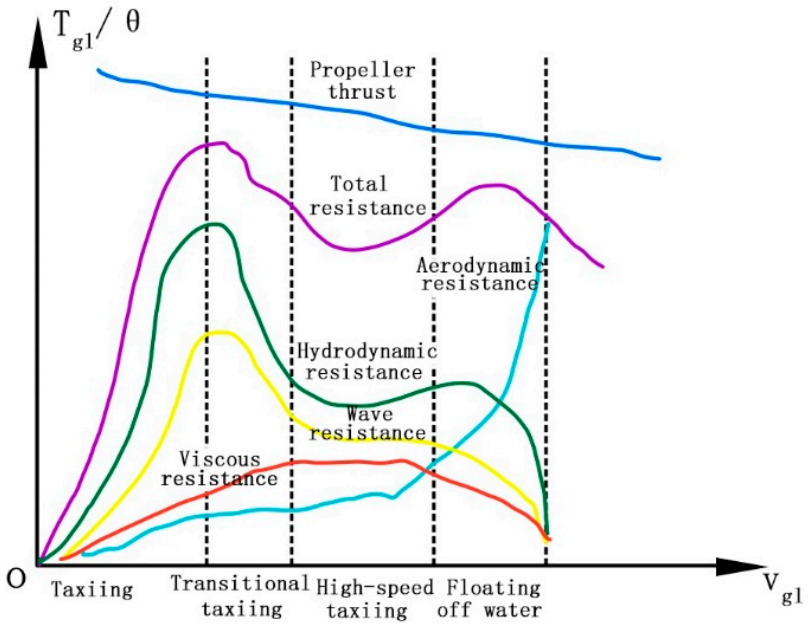

Figure 1. Hydrodynamic resistance and aerodynamic resistance [13].

During the take-off taxiing of a seaplane, the taxiing stage marks the initial phase. It operates at relatively lower speeds, usually maintaining a lower speed range while gliding on the water surface. The resistance experienced by the electric seaplane primarily originates from water surface resistance. As the electric seaplane glides on the water surface, this resistance increases, challenging acceleration [27]. Friction and resistance from the water surface significantly impact the electric seaplane's steering and acceleration.

Transitional taxiing represents the second phase. Its initial speed is typically low, gradually increasing over time. The primary resistances encountered by the electric seaplane include water surface resistance and aerodynamic resistance. Water surface resistance escalates with speed, while aerodynamic resistance remains relatively minor during this phase because a significant portion of the electric seaplane's body remains in contact with the water surface.

High-speed taxiing is the third phase. Typically, the electric seaplane progressively gains speed to attain take-off velocity while floating on water. Regarding its resistance characteristics, the electric seaplane is primarily influenced by aerodynamic resistance and a minimal amount of hydrodynamic resistance. As speed increases, aerodynamic resistance gradually rises. Water surface resistance is relatively small since much of the electric seaplane's body is already lifted from the water.

Floating off water represents the final phase. The electric seaplane achieves the required take-off speed and initiates departure from the water surface. Once the electric seaplane reaches sufficient velocity, it generates adequate lift to leave the water surface. As the seaplane departs from the water, surface resistance diminishes rapidly, and aerodynamic resistance becomes dominant [28].

Generally, seaplanes consume more energy during take-off than land-based planes. Seaplanes encounter resistance from the water surface during take-off, and due to the considerable water surface resistance, this necessitates higher thrust and energy consumption for lift-off. Additionally, seaplanes typically require longer take-off distances due to the significant water surface resistance. This implies they demand increased thrust and time to attain take-off speed, escalating energy consumption. By establishing a mathematical model for energy losses and conducting numerical calculations for seaplane energy consumption,

we can undertake computational analysis to optimize energy consumption for individual flight missions.

Reference [29] optimized the floats based on aerodynamic and hydrodynamic characteristics and conducted validation calculations for the power required by the EPU at the drag peak nodes. Reference [30] proposed a semi-theoretical, semi-empirical formula for the taxiing resistance of seaplanes. These studies qualitatively or within a certain error margin revealed the hydrodynamic characteristics of seaplanes during takeoff. Given the limited reference value of existing results, a more precise analysis is needed [31].

In this study, we introduce a novel approach to optimizing the energy efficiency of the EPUs in electric seaplanes during their take-off phase. By developing a comprehensive mathematical model and conducting prototype tests, we demonstrate a significant reduction in energy consumption by adjusting the propeller pitch angle. In addition, we have implemented a gradient algorithm that is capable of rapidly determining the optimal propeller pitch angle for various models of electric seaplanes, taking into account the diverse conditions of aquatic take-off environments and flight missions. This contribution enhances the energy efficiency of EPUs.

2. Analysis of the Electric Power Unit

2.1. The Composition of the Electric Power Unit

The electric power unit mainly consists of components such as the motor, motor controller, motor mounts, propeller, power-integrated display, comprehensive power system, throttle lever, and control switches. The power-integrated display also incorporates supplementary system information, providing control and communication functionalities, including cooling fans, temperature-monitoring systems, sensors, and communication devices, to support the system's regular operation. The electric motor serves as the core component of the EPU, converting electrical energy into mechanical energy. It propels the seaplane forward by driving the propeller assembled with an electric motor to provide thrust. The type and specifications of the electric motor depend on the seaplane's requirements and design, commonly utilizing permanent magnet synchronous motors.

The motor controller is a crucial part of the EPU, managing the flow of electricity to the electric motor, controlling thrust output, and monitoring and protecting the system's operational status. Depending on the requirements of the electric seaplane and flight conditions, pilots control the throttle lever and control switches. They adjust the motor's speed and power output with real-time feedback from the power display.

The comprehensive power system comprises the power battery and electrical transmission equipment, primarily providing electrical energy to the electric motor. It includes components like the power battery pack, power management system, cables, and connectors. Electrical energy is stored in the battery and transmitted to the electric motor via cables. The power battery needs to be charged on the ground. Determining the power battery system's lifespan is based on the actual capacity declining to 80% of its nominal capacity. Capacity verification is required every 200 cycles, and replacement is necessary when the capacity falls below the degradation limit. A schematic diagram of the RX1E-S electric seaplane EPU is shown in Figure 2.

As the maximum power consumption of the battery occurs during the take-off phase of the seaplane, this paper necessitates an analysis of the efficiency and energy consumption during the take-off phase.

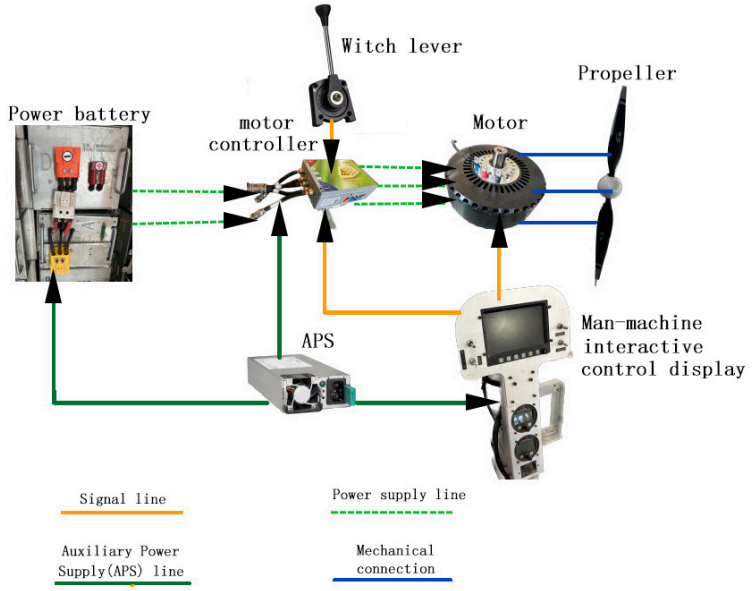

Figure 2. Electric power unit composition.

2.2. Propeller Analysis and Model Building

Electric seaplanes often utilize direct-drive motors to power fixed-pitch propellers, primarily because fixed-pitch propellers simplify design and manufacturing processes and reduce the weight and complexity of the aircraft. Their design and performance are crucial for battery efficiency. The design of fixed-pitch propellers for electric seaplanes needs to consider performance requirements both on the water surface and in the air. Factors such as the propeller's pitch angle, shape, and rotational speed directly influence the electric seaplane's energy consumption and take-off performance. By optimizing the design of fixed-pitch propellers, it is possible to reduce aerodynamic resistance and enhance thrust efficiency, thereby reducing the energy consumption of the electric seaplane, increasing the flight range for individual missions, and improving the overall performance and efficiency of the electric seaplane.

The energy source for electric seaplanes is derived from the battery system, thus necessitating proper management and optimization of power usage. The alignment between propeller thrust and power is crucial in enhancing battery energy efficiency. It minimizes power consumption by selecting the optimal propeller pitch angle to match the rotational speed and thrust output, thereby extending the seaplane's endurance.

The propeller efficiency of an electric seaplane on the water surface significantly impacts its overall energy efficiency. The design and performance of the propeller affect the seaplane's propulsion and maneuverability on water. By optimizing the shape and rotational speed of the propeller, it is possible to enhance its efficiency, thereby reducing energy consumption.

In contemporary aviation research, the theoretical calculation of propeller flow field parameters involves momentum theory, blade element theory, and vortex theory [13,14]. Specifically for our application on the RX1E-S electric seaplane, we have designed a three-blade fixed-pitch propeller, as shown in Figure 3. The RX1E-S electric seaplane utilizes a three-blade composite, ground-adjustable pitch carbon fiber propeller, with blade model PROC03-68 and hub model 3-RT2-A, manufactured by Shenyang Stana Aviation Technology Co. The propeller, directly driven by the motor without a reduction gear, is mounted using a flange plate and rotates clockwise when viewed from the cockpit. It has a diameter of 68 inches (1.73 m) and weighs 3.55 kg. With a blade tip angle set at 9 degrees, at 2346 rpm, the propeller generates a thrust of 181.5 kg and requires a motor input power of 46 kW. Under maximum power of 68 kW, the propeller's measured ground static thrust exceeds 240 kg, as detailed in Table 1. This design decision is rooted in a comprehensive

aerodynamic analysis, taking into account factors such as efficiency, reliability, and simplicity of operation. The specific parameters of the propeller, including its pitch angle, shape, and rotational speed, are custom-tailored to meet the particular requirements of the RX1E-S model, ensuring optimal performance in both aquatic and aerial environments. This approach is in line with our objective of achieving a balance between performance and practicality, particularly in the unusual operational context of electric seaplanes.

(**a**) (**b**)

Figure 3. The propeller of RX1E-S electric seaplane: (**a**) experimental prototype model; (**b**) prototype bench test.

Table 1. Static performance data of three-blade composite propeller (tip 9 degrees).

Rotation Speed/(r·min^{-1})	Trust/kg	Torque/(N·m)	Power/kW
1900	120	110	21.8
2400	210	210	52.7
2600	240	250	68.0

This article constructs a model for fixed-pitch propellers based on the general method of propeller performance calculation. Since the pitch angle of a fixed-pitch propeller is constant, its performance curve is a quadratic curve. To determine the performance curves of a fixed-pitch propeller at different pitch angles and to select the optimal propeller pitch angle, the following formula can be used for calculation:

$$\begin{cases} \lambda = \frac{v}{2n_p R_p} \\ C_T = \frac{T_p}{16\rho n_p^2 R_p^4} \\ T_p = \frac{32\rho n_p^3 R_p^5 \beta \eta_{net}}{v} \\ W_p = 32\beta\rho R_p^5 n_p^3 \end{cases} \quad (1)$$

where W_P stands for the power requirement of the propeller; T_P represents the propeller thrust; C_T characterizes the influence of factors such as the pitch angle, airfoil, and number of blades on the propeller thrust; β is the power coefficient of the propeller; λ signifies the advance ratio; v represents the incoming flow velocity; ρ stands for air density, given that for low-altitude flights below 3000 m, the air density for seaplanes can be approximated as 1.29 kg/m^3; n_P stands for the propeller rotational speed; and R_P denotes the propeller radius. The C_T coefficients at these different propeller pitch angles were determined through wind tunnel testing. The characteristics of λ with respect to the variation in

propeller rotational speed and incoming flow velocity can be determined through propeller wind tunnel experiments.

After determining the propeller's material and blade count, adjusting its pitch angle can modify its high-efficiency operating speed. The pitch angle directly impacts the propeller's thrust output. A larger pitch angle typically generates higher thrust, suitable for phases requiring greater thrust, such as take-off and climb. However, this scenario demands higher power to drive the propeller, potentially affecting fuel efficiency and endurance. Conversely, a smaller pitch angle can reduce thrust, which suits situations needing lower thrust, such as high-speed flight and cruising. At this point, the relative speed of the propeller blades is lower, aiding in reducing aerodynamic drag. Hence, adjusting the pitch angle allows control over the propeller's thrust within a specific range.

We calculated the variations in thrust by substituting five typical C_T coefficients into Equation (1), as illustrated in Figure 4. At lower rotational speeds, the variation in thrust is relatively gradual, exhibiting a progressive characteristic. Consequently, these less pronounced changes are omitted in Figure 4. At higher rotational speeds, the thrust at a constant speed consistently shows a trend of gradual increase with the enlargement of the C_T. The performance characteristics of the propeller as a function of its C_T provide valuable insights and challenges for the design and performance optimization of seaplanes.

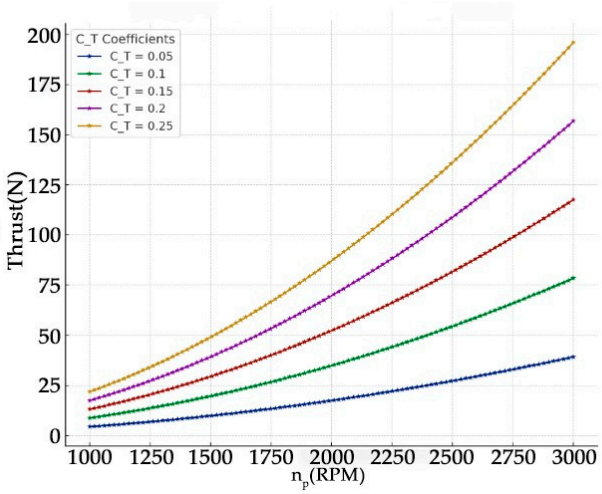

Figure 4. Thrust variation with different C_T coefficients.

We can calculate the propeller efficiency using Equation (2):

$$\eta_{net} = \frac{C_T}{\beta}\lambda \tag{2}$$

where the pitch angle is fixed, β and η_{net} are functions of λ, and the propeller's efficiency is closely related to the pitch angle. The propeller can achieve its highest efficiency within a specific range of pitch angles, known as its high-efficiency operating speed range. The propeller can generate maximum thrust within this range with minimal power output. Adjusting the pitch angle can change the position of the high-efficiency operating speed range within a specific range.

Overall, these data indicate that selecting the appropriate pitch angle is crucial for the performance of an electric seaplane. Therefore, a careful balance between performance requirements, power system capabilities, and the motor's operating range is necessary to determine the optimal pitch angle. Further research and analysis will aid in a better understanding of the effects of different pitch angles on electric seaplane performance, enabling better alignment with specific mission and flight requirements.

3. Dynamic Characteristic Analysis of the Take-Off Phase

The take-off phase of the electric seaplane can be divided into two stages: the take-off taxiing stage and the climbing stage, as illustrated in Figure 5. The take-off taxiing stage is characterized by slower speeds and the floats sliding on water, resulting in a more complex force analysis. We further divide this stage into four phases—taxiing, transitional taxiing, high-speed taxiing, and floating off water—which will be analyzed in detail and modeled mathematically in Section 3.2. The climbing portion is relatively simpler; the climbing phase of the electric seaplane, compared to land-based aircraft, includes additional aerodynamic drag due to the floats but is similar overall. This will be thoroughly analyzed and mathematically modeled in Section 3.3.

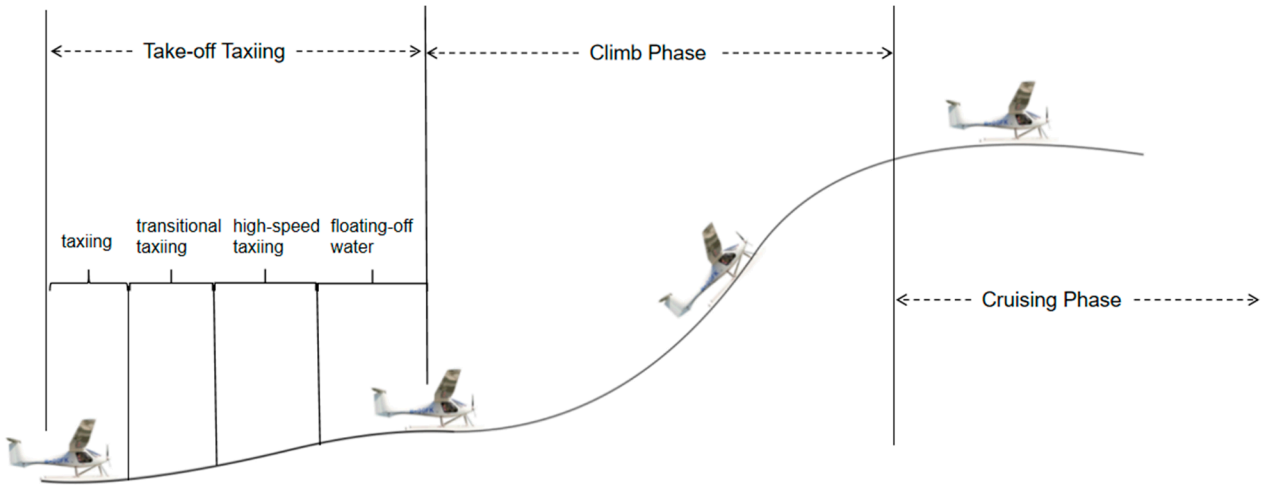

Figure 5. Electric seaplane's take-off phase.

3.1. Electric Seaplane Force Analysis

The seaplane's take-off taxiing phase comprises four stages: taxiing, transitional taxiing, high-speed taxiing, and floating off water. Assuming the seaplane's speed is 0 upon entering the taxiing phase and reaches a speed of v_{LOF} during the skimming take-off stage, the seaplane lifts off the water and enters the climbing phase.

During the take-off phase of the seaplane, various forces affect the seaplane, including its weight, propeller thrust, aerodynamic lift, aerodynamic drag, buoyancy, and hydrodynamic drag. A preliminary force analysis is depicted in Figure 6.

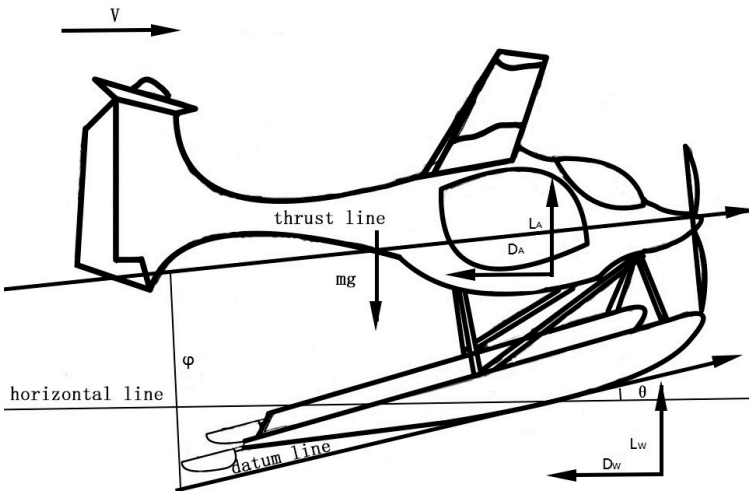

Figure 6. Force on the seaplane during the take-off phase.

Here, θ represents the pitch angle of the seaplane, which denotes the angle between the datum line and the horizontal plane. φ represents the angle between the electric power unit's thrust line and the seaplane's lower structure line. This value can be approximately determined after the seaplane is configured. m signifies the take-off mass of the seaplane, which is the total weight carried by the seaplane during take-off. Take-off mass is a critical parameter that significantly impacts the seaplane's take-off performance, fuel consumption, and range. Based on these parameters, we can derive the key formula that affects the performance of the seaplane, as shown below:

$$\begin{cases} L_W = mg - T_P \sin(\theta + \varphi) - L_A \\ T_p \cos(\theta + \varphi) = ma + D_W + D_A \end{cases} \tag{3}$$

where T_P represents the thrust output of the propeller during the take-off phase; D_A stands for aerodynamic drag; D_W represents hydrodynamic drag; L_A denotes aerodynamic lift; and L_W signifies hydrodynamic lift.

3.2. Calculation of Energy Consumption during the Take-Off Taxiing Phase

Based on the distinct features of the take-off taxiing phase, it is divided into four stages: taxiing, transitional taxiing, high-speed taxiing, and floating off water.

Taxiing is the initial stage of the take-off taxiing phase and exhibits distinctive characteristics. In this phase, the hydrodynamic lift appears negative due to the lower cruising speed, resulting in significantly reduced aerodynamic forces compared to hydrodynamic forces. Consequently, there is a need to augment the buoyancy to balance a considerable portion of the seaplane's weight. For most seaplanes, the weight compensation is primarily provided by hydrodynamic lift, with buoyancy playing a major role in supporting the seaplane against gravity. In this calculation, the impact of aerodynamic forces on the seaplane can be neglected.

During transitional taxiing, a resistance peak corresponding to the 'lift-off speed' exists. At this stage, an air cushion phenomenon occurs at the bottom of the float, reducing the sliding area of the aft body and subsequently decreasing the hydrodynamic forces and moments acting on it. To maintain balance, the hydrodynamic force on the front body increases continuously, leading to a rapid increase in the total hydrodynamic moment of the seaplane. During this process, the waterline height first increases and then decreases.

During the high-speed taxiing phase, an electric seaplane experiences a rapid increase in velocity while floating on the water's surface. The drag characteristics of this type of aircraft are primarily influenced by aerodynamic resistance, with hydrodynamic resistance being relatively minor in comparison. As the speed increases, the aerodynamic resistance gradually escalates. Since most of the aircraft's body is above the water surface at this stage, the resistance from the water is comparatively low.

During the floating off water, as the taxiing speed gradually increases, the seaplane's pitch angle also rises, causing the water flow to scour the hull and increasing hydrodynamic skimming resistance. Simultaneously, aerodynamic resistance continues to mount, forming a second resistance peak. However, hydrodynamic resistance rapidly decreases soon after until it reaches zero as the seaplane departs the water. This signifies the conclusion of the seaplane's take-off taxiing phase.

In this section, we will provide a detailed analysis of the mathematical models used for calculating the energy consumption of each of these four stages.

3.2.1. Taxiing

During this stage, the seaplane's taxiing behavior is similar to that of a ship navigating through water. Hence, corresponding calculations can be carried out using methods applicable to low-speed ship navigation [32].

The hydrodynamic resistance D_W during the taxiing comprises two components: viscous resistance, R, and wave-making resistance, R_W.

C_f represents the water's friction coefficient calculated according to the Prandtl–Von Kármán formula, with R representing the viscous resistance. The specific calculation formula is as follows:

$$\begin{cases} C_f = \frac{0.455}{(\lg \mathrm{Re})^{-2.58}} \\ R = C_f \frac{\rho_w v_w^2}{2} B N_p \\ R_e = \frac{\rho_w v_w B}{\mu_w} \end{cases} \tag{4}$$

where R_e represents the Reynolds number and B stands for the float width, which can be determined based on the parameters of the seaplane. N_P denotes the number of floats, and v_W denotes the seaplane's speed relative to the water. For calm water or water with relatively slow currents, the seaplane's speed can be used for calculations. μ_W represents the viscosity coefficient of water, and ρ_W denotes the density of water. The specific values of μ_W and ρ_W are determined based on the aquatic environment conditions wherein the electric seaplane frequently takes off.

We can define coefficient K_0 based on the formula for calculating wave-making resistance and denote the acceleration due to gravity g = 9.8 m/s^2:

$$K_0 = \frac{g}{v_W^2} \tag{5}$$

We can then establish a coordinate system for the pontoon, where $\xi = (x, y, z)$ represents the source point coordinates on the pontoon surface. The potential function for the sources and sinks can be expressed as follows:

$$\begin{cases} \varphi(x_1, y_1, z_1) = \frac{1}{4\pi} \int\limits_S \sigma(\vec{\xi}) G(x_1, y_1, z_1, \vec{\xi}) dS - \frac{1}{4\pi K_0} \oint\limits_{C_W} \sigma(\vec{\xi}) \cos(x, n) G(x_1, y_1, z_1, \vec{\xi}) dw \\ \sigma(x, 0, z) = -2v f_x(x, y) \end{cases} \tag{6}$$

where S_w denotes the wet surface area of the pontoon submerged in still water, σ represents the potential strength distributed on the pontoon surface, c_W stands for the intersection between the net water surface and the pontoon surface, and $\cos(x, n)$ refers to the cosine of the angle between the normal to the pontoon surface and the x-axis. Here, $dw = ds \cdot \sin(y, n)$, where ds_w is an elemental quantity along the waterline. f_x represents the equation of the pontoon surface, and G signifies Green's function.

The term κ is mathematically defined as an intermediate variable and physically denotes the angle between the direction of the propagating elemental wave (a sinusoidal long wave) and the forward direction of the pontoon. The calculation method for wave-making resistance is as follows:

$$\begin{cases} R_w = \frac{N_p K_0^2}{\pi \rho_w v^2} \int_0^{\frac{\pi}{2}} \sec^5 \kappa |H_1(K_0 \sec^2 \kappa, \kappa)|^2 d\kappa \\ H_1(K_0 \sec^2 \kappa, \kappa) = \int_S p e^{iK_0 \sec^2 \kappa \omega} dS \\ \omega = x \cos \kappa + y \sin \kappa \\ p = v \rho_w \varphi(x_1, y_1, z_1) - \rho_w g z \end{cases} \tag{7}$$

H_1 represents the Kochin function, p represents the pressure distribution on the pontoon surface, and i represents the imaginary unit.

The water resistance during taxiing, D_W, is obtained by summing the viscous resistance R and wave resistance R_W.

$$D_W = R + R_W \tag{8}$$

The calculation method for the required thrust output of the propeller is determined by Equation (3), and power calculation is performed according to the formula for thrust power. According to the momentum theory, the propeller's thrust output and power requirements can be calculated using Equation (1).

The total energy consumption of the electric seaplane taxiing is computed using the following formula:

$$E_{g\_1} = \frac{\int_0^{t_{g\_1}} w_{p\_1} dt}{\eta_m \eta_c \eta_{net}} \tag{9}$$

The formula presents E_{g_1} as the total energy consumption during taxiing, t_{g_1} as the time duration of taxiing, and w_{p_1} as the power required for the seaplane's operation during this stage. Here, η_m, η_c, and η_p denote the efficiencies of the seaplane's motor, controller, and propeller. These efficiencies can be acquired from the flight test data obtained.

3.2.2. Transitional Taxiing

The primary characteristic of this stage is the rapid increase in pitch angle and reduction in immersion. While the aerodynamic resistance of the electric seaplane begins to increase rapidly, the hydrodynamic resistance still significantly surpasses the aerodynamic resistance due to the air cushion phenomenon at the bottom of the float. The computation for this aspect can be conducted using models for high-speed boat navigation.

For the water's friction coefficient C_{f1} during this stage, the Sarpkaya formula can be applied for calculation:

$$\frac{0.242}{\sqrt{C_{f1}}} = \lg(\mathrm{Re} \cdot C_{f1}) \tag{10}$$

The remaining calculation methods are similar to the taxiing stage, computed using Equations (1), (3) and (5)–(8).

The electric seaplane's total energy consumption during transitional taxiing is calculated using the following formula.

$$E_{g\_2} = \frac{\int_0^{t_{g\_2}} w_{p\_2} dt}{\eta_m \eta_c \eta_{net}} \tag{11}$$

The formula presents E_{g_2} as the total energy consumption during the transitional taxiing, while t_{g_2} signifies the duration of the transitional taxiing and w_{p_2} is the power required for the seaplane's operation during this stage.

3.2.3. High-Speed Taxiing

During high-speed taxiing, the floating body rises, creating an air cushion after the step, thereby increasing the air cushion area. This further reduces the submerged area, whereby the hydrodynamic resistance decreases slowly. Simultaneously, as the speed increases, the aerodynamic resistance starts to escalate.

D_A represents the aerodynamic resistance of the seaplane and can be expressed as follows. S is the wing area; C_D is the aerodynamic drag coefficient.

$$D_A = \frac{\rho S C_D}{2} v^2 \tag{12}$$

Let D_s denote the total resistance experienced by the seaplane during high-speed taxiing. R_1 and R_{W1}, representing the viscous resistance and wave-making resistance during this phase, respectively, are determined by Equations (1), (3), (5)–(8) and (10):

$$D_s = D_A + R_1 + R_{W1} \tag{13}$$

The power is computed according to the formula for calculating power using thrust (Equation (1)). The total energy consumption during the high-speed taxiing within the seaplane's journey is calculated using the following formula:

$$E_{g\_3} = \frac{\int_0^{t_{g\_3}} w_{p\_3} dt}{\eta_m \eta_c \eta_{net}} \tag{14}$$

The formula presents E_{g_4} as the total energy consumption during the high-speed taxiing, while t_{g_3} signifies the duration of high-speed taxiing and w_{p_3} is the power required for the seaplane's operation during this stage.

3.2.4. Floating off Water

In this phase, due to the flying speed of the seaplane being 0.8 to 1 times the stall speed and with the increase in wing lift reducing the submerged portion of the float to zero, the seaplane rapidly ascends.

The Fraude formula is the water resistance calculation formula:

$$D_{ww} = \frac{\rho_w g}{1000}\left\{0.1392 - \frac{2.258}{(2.68 + l_b)}\right\}\{1 + 0.0043(15 - t_w)\}Sv^{1.825} \tag{15}$$

where D_{ww} represents the hydrodynamic resistance, l_b represents the float's length, and t_w denotes the water temperature.

The equation for the calculation of aerodynamic resistance is similar to that of the high-speed sliding phase. The water resistance is calculated using Equation (15)

According to the power calculation Formulas (1), (3) and (5)–(8), the electric seaplane's total energy consumption during floating off water is computed using the following Equation:

$$E_{g\_4} = \frac{\int_0^{t_{g\_4}} w_{p\_4} dt}{\eta_m \eta_c \eta_{net}} \tag{16}$$

The formula presents E_{g_4} as the total energy consumption during the floating off water, while t_{g_4} signifies the duration of floating off water and w_{p_4} is the power required for the seaplane's operation during this stage.

3.3. Calculation of Energy Consumption during the Climbing Phase

Once the floats of the electric seaplane leave the water surface, the seaplane enters the climbing phase. The climb of a seaplane is broadly similar to that of a land-based aircraft. During the climbing phase, the propeller continues to operate at high power, with the output thrust remaining constant. Assuming that the aircraft's climb altitude and angle are fixed, and referencing the energy demand calculation for the EPUs of land-based aircraft, the energy requirement of the EPU for a seaplane during the climbing phase can be approximated as follows:

$$\begin{cases} E_{g\_5} = \int_0^{\frac{2H\cot\gamma}{v_{cr}+v_{LOF}}} \frac{16 C_T \rho R_P^4 n_P^2 v_{cl}\cos\gamma}{\eta_m \eta_c \eta_{net}} dt \\ v_{cl} = v_{LOF} + \frac{(v_{cr}^2 - v_{LOF}^2)\tan\gamma}{2H} t \\ \eta_{net} = \frac{C_T v_{cl}}{2 n_P R_P \beta} \end{cases} \tag{17}$$

herein, E_{g_5} represents the energy demand of the seaplane during this phase, v_{cr} denotes the cruising speed of the seaplane, v_{cl} is the velocity of the seaplane, γ indicates the climb angle, and H refers to the cruising altitude of the seaplane.

4. Optimization Method

The optimization of the propeller during the take-off phase of electric seaplanes is crucial for achieving enhanced energy efficiency. In contrast to land-based planes, the take-off process of seaplanes is influenced by various external forces, including water resistance and aerodynamic drag. Therefore, a systematic energy consumption model for the take-off phase has been established. By analyzing key aspects such as motor efficiency, propeller design, and control system efficiency, and optimizing the energy efficiency of the EPU during the take-off phase of seaplanes, we will focus on the following optimization methods:

The propeller experiences the highest thrust demands during the seaplane's take-off phase. Different pitch angles have different performance. We aim to optimize the propeller's pitch angle to enhance the efficiency and performance of the propulsion system. We will determine the optimal pitch angle configuration through prototype experiments and with seaplane design requirements, ensuring that the propeller's thrust output meets minimum requirements during take-off while improving energy efficiency. In the take-off phase, precisely matching the electric motor's power output and the propeller's rotation speed is necessary. This is achieved by managing the electric motor's power and propeller control strategies to enable high-efficiency operation during take-off.

The established objective function for optimizing the EPU is as follows:

$$E_{\min} = \min(\sum_{x=1}^{5} E_{g\_x}) \tag{18}$$

The pitch angle of the propeller's efficient rotational speed point can be adjusted to achieve the minimum energy consumption of the EPU when a seaplane completes one take-off mission profile. The efficiency optimization design method for the EPU of a seaplane during take-off is outlined as follows:

Step 1: Determine the minimum pitch angle ($\alpha_{\min}$) and maximum pitch angle ($\alpha_{\max}$) of the propeller.

Step 2: Set the counter 'n' to 1 and the propeller's pitch angle to the minimum pitch angle ($\alpha_{\min}$). Calculate the energy consumption ($E_{es}[1]$) of the EPU when completing one flight mission.

Step 3: Calculate the gradient of the energy consumption ($\partial E_{es}/\partial\alpha$) at the current pitch angle.

Step 4: Increase the counter 'n'. Update the pitch angle to $\alpha_n = \alpha_{n-1} - \tau(E_{es}/\partial\alpha)$, where τ is a small learning rate factor.

Step 5: Calculate the energy consumption ($E_{es}[n]$) of the EPU for the updated pitch angle.

Step 6: Determine if the change in energy consumption is below a certain threshold or if α_n is less than or equal to the maximum pitch angle $\alpha_{\max}$. If not, return to step 3.

Step 7: Once the convergence criterion is met, set α_{opt} to the current pitch angle α_n. $E_{\min}$ is the corresponding minimum energy consumption.

In this method, the maximum and minimum values of the propeller pitch angle serve as the boundary conditions for gradient optimization calculations and can generally be roughly determined through experimentation. When conducting gradient optimization, the initial value can be set as either the upper or lower boundary, as the optimal pitch angle is typically contained within these boundaries. The search is conducted in a consistent direction. Additionally, the learning rate factor is determined through a trial-and-error process. It is common to start with a smaller value and then adjust it based on performance. It is important to note that a smaller learning rate does not lead to entrapment in a local optimum in this context.

By employing a gradient-based optimization method and gradually adjusting the pitch angle of the propeller within a specified range, the energy consumption can be effectively calculated. This method dynamically updates the pitch angle based on the rate of change in energy consumption with respect to the pitch angle (i.e., the gradient), thereby identifying the optimal pitch angle α_{opt} that minimizes energy consumption. Such a method allows for a more precise approximation of the minimal energy consumption, leading to the determination of the optimal propeller pitch angle configuration.

Adopting this gradient-based optimization strategy significantly enhances the energy efficiency of seaplanes during the take-off phase, enabling more efficient take-off performance.

5. Prototype Experiment and Method Verification

This study aims to optimize the efficiency of the EPU of an electric seaplane to reduce energy consumption during individual flight missions. The feasibility and accuracy of the proposed optimization method were verified through actual tests on an RX1E-S electric seaplane.

In this section, the RX1E-S seaplane was chosen as the platform of verification, and its design parameters were determined. Numerical calculations were conducted to identify the optimal propeller pitch angle required for the flight mission to achieve minimal energy consumption and maximal efficiency.

Subsequently, prototype flight tests were conducted using the calculated propeller pitch angles for the same flight mission in the same body of water. The accuracy and reliability of the proposed optimization method were validated through the comparison of experimental data with numerical results, proving its effectiveness in practical applications.

Section 5.1 will provide a detailed introduction to the RX1E-S seaplane. Section 5.2 will extensively discuss the flight mission and the results of optimization. In Section 5.3, an analysis and discussion will be conducted on the experimental results, numerical calculations, and the observations made during the actual test flights of the seaplane.

5.1. RX1E-S Two-Seater Electric Seaplane

The RX1E-S seaplane is an electric, single-engine aircraft featuring a fixed-pitch, tractor configuration propeller, side-by-side two-seater arrangement, high-aspect-ratio cantilever wing, and T-tail layout. The landing gear consists of twin floats. The airframe is constructed from an integrated carbon fiber composite material, classifying it as a light sport aircraft. The primary systems of the RX1E-S electric seaplane include an electric propulsion system, floats, a control system, avionics, and support equipment for waterborne takeoff and landing operations.

The experimental prototype is depicted in Figure 7.

(**a**) (**b**)

Figure 7. Experimental prototype of the RX1E-S electric seaplane. (**a**) Experimental prototype model; (**b**) prototype flight test.

The primary parameters of the experimental prototype include fuselage length, fuselage height, wingspan, and wing area, as detailed in Table 2 and shown in Figure 8. The performance indicators of the RX1E-S electric seaplane are shown in Table 3.

The experimental prototype employs a lightweight air-cooled permanent magnet synchronous electric motor, renowned for its exceptionally high continuous torque density and efficiency, suitable for direct propeller drive. The primary performance parameters of the electric motor are detailed in Table 4.

Table 2. Overall parameters of RX1E-S.

Parameter Name	Parameter Value
Aircraft length/m	6.78
Aircraft height/m	2.93
Wingspan/m	14.5
Wing area/m^2	12
Buoy spacing/m	2.2
Buoy length/m	4.67
Single buoy volume/m^3	0.6
Buoy mounting angle/(°)	−1.5
Motor tension line angle/(°)	0
Propeller diameter/m	1.75

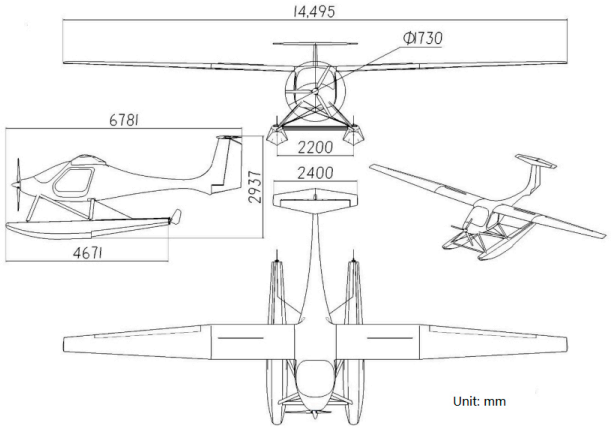

Figure 8. Dimensional view of the RX1E-S seaplane.

Table 3. RX1E-S electric seaplane performance indicators.

Parameter Name	Reference Value
Technical index/(km·h^{-1})	165
Stalling speed/(km·h^{-1})	90
Cruising altitude/m	1000
Cruising speed/(km·h^{-1})	100
Service ceiling/m	3000
Duration of flight/min	≥75
Maximum service overload/g	+3.33/−1.6
Maximum take-off weight/kg	650

Table 4. Motor parameter.

Parameter Name	Parameter Value
Rated power	60 kW
Rated speed	2450 r/min
Rated torque	235 Nm
Maximum speed	3600 r/min
Maximum torque (30 s)	300 Nm
Class of protection	IP66
Cooling mode	Air cooling
Operating ambient temperature	−30°~50°
Humidity	0~100%
Altitude	<5000 m
Cooling medium temperature under rated operating conditions	30°
Cooling air velocity (axial)	>25 m/s
Weight	26 kg

5.2. Flight Mission Profile and Optimization Results

A single flight mission for an electric seaplane includes two phases: the take-off taxiing phase and the climbing phase. During the take-off taxiing phase, the seaplane must overcome the dual resistance of water and air. This part of the mission is considered complete upon reaching the seaplane's stall speed. The climbing phase, similar with land-based aircraft, is influenced by the air resistance of the distinctive floats of the seaplane. This part of the mission aims to reach a predetermined cruising altitude and speed for the flight mission.

As per the optimization method mentioned in Section 4 and the mathematical model provided in Section 3, we optimized the propeller pitch angle for the RX1E-S electric seaplane. It is important to note that power limitations were incorporated into the calculations for propeller pitch angles above 18.5°. We calculated the optimal propeller pitch angle for the lowest energy consumption during the take-off taxiing phase to be 18.8° and for the climbing phase to be 15.1°. The optimal propeller pitch angle for the lowest total energy consumption of a single take-off mission was calculated to be 17.2°, as shown in Figure 9. For the take-off taxiing phase, due to multiple resistances, a greater propeller thrust is required, meaning higher propeller efficiency at larger pitch angles, resulting in shorter taxiing distance and a shorter time to reach takeoff speed. In the climbing phase, as the RX1E-S electric seaplane gradually increases its speed to cruising, it is mainly affected by air resistance and gravity. At smaller pitch angles, the seaplane's total power is lower, and due to its slower climbing speed, the time taken to reach the required altitude and speed for the flight mission is longer, increasing energy consumption.

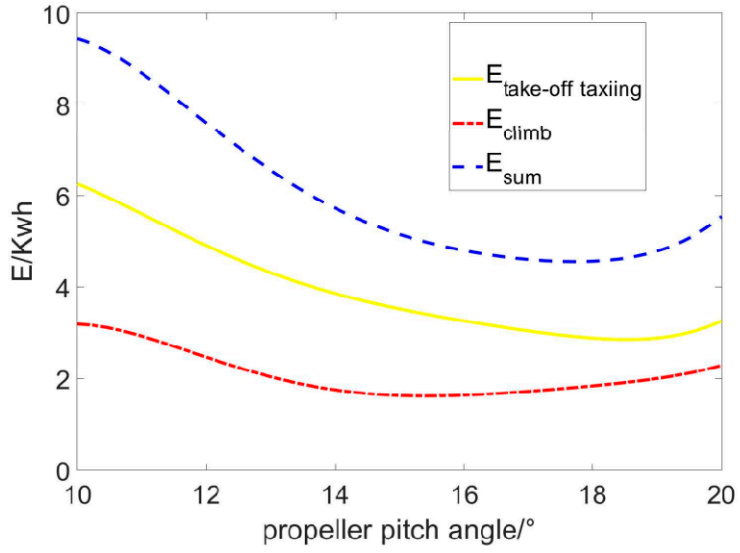

Figure 9. Energy consumption at different blade angles.

We calculated the lowest energy consumptions for the take-off taxiing phase, climbing phase, and the entire single takeoff mission to be 2.9 kWh, 1.6 kWh, and 4.9 kWh, respectively. It was found that for a single flight mission, using the optimal propeller pitch angle for the entire mission reduces the energy consumption by approximately 4.4% compared to using the optimal pitch angle for the take-off taxiing phase, and by about 8.1% compared to the optimal pitch angle for the climbing phase.

5.3. Verification and Discussion of Optimization Effects and Test Results

Flight experiments with different propeller pitch angles were conducted on the RX1E-S electric seaplane. Five sets of propellers were selected for the experiments, with pitch angles of 11°, 13°, 15°, 17°, and 19°, respectively. The experiments involved piloting the seaplane under the same meteorological conditions and over the same body of water to perform identical flight tasks. The following experimental data were obtained, as shown in

Figure 10. In the propeller tests of the RX1E-S two-seater electric seaplane, different pitch angles significantly impacted torque. Higher pitch angles produced greater torque, which offers stronger accelerating ability but increases the load on the motor and power system. Moderately reducing the pitch angle to around 17° slightly decreased torque. Lower pitch angles further reduced torque, making them suitable for specific scenarios requiring lower torque. Overall, different pitch angles provided an optimal balance of torque under special experimental conditions. This optimization of pitch angles directly contributed to enhanced efficiency and performance.

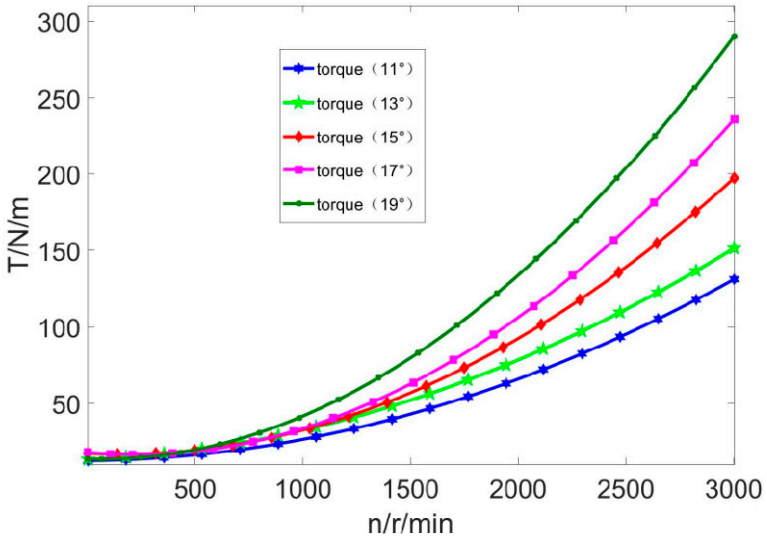

Figure 10. Torque variation curve with pitch angle.

However, a notable aspect of this part of the experiment was that during the flight experiments with a 19° propeller pitch angle, the thrust generated did not align with the expectations introduced in Section 2. The thrust at a 19° pitch angle did not surpass that of lower pitch angles. To address this, we conducted performance tests on the RX1E-S electric seaplane during the climbing phase, specifically during periods of relatively stable aerodynamic resistance. These tests were analyzed, as shown in Figures 11–13.

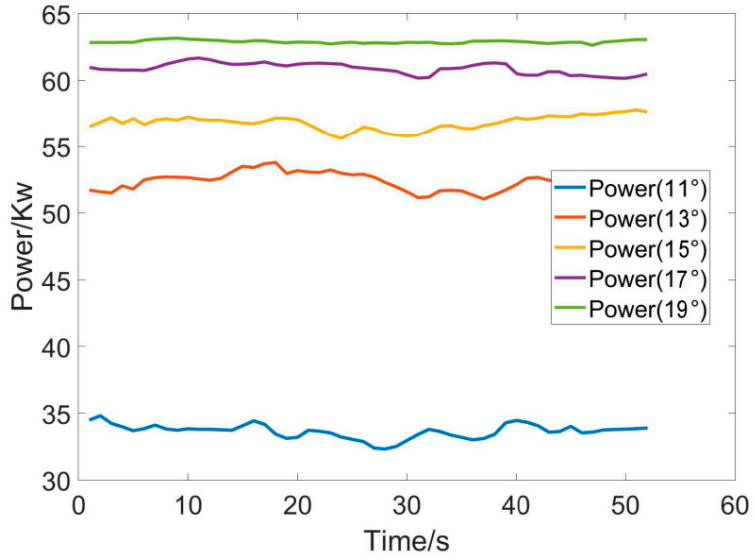

Figure 11. Power at different propeller pitch angles for the RX1E-S seaplane.

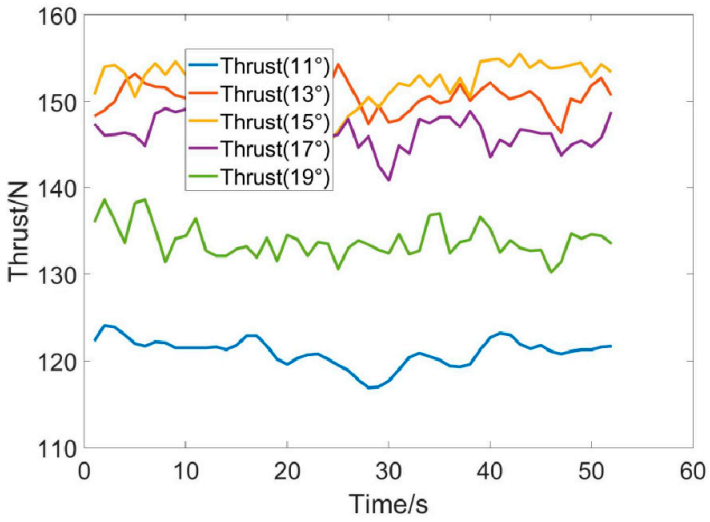

Figure 12. Thrust at different propeller pitch angles for the RX1E-S seaplane.

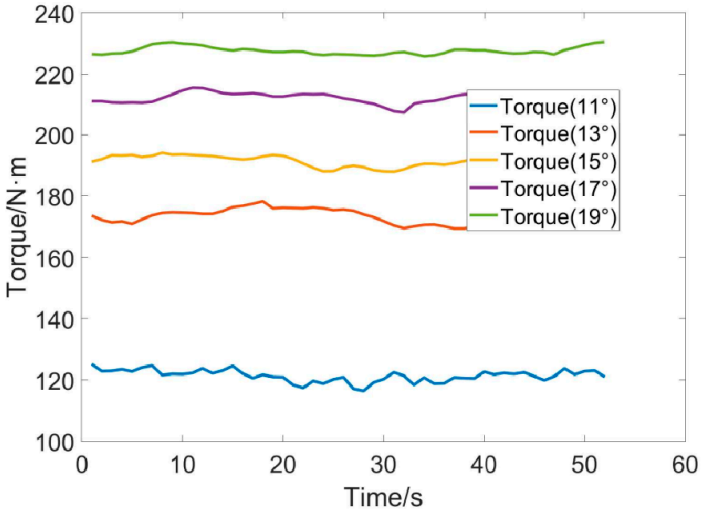

Figure 13. Torque at different propeller pitch angles for the RX1E-S seaplane.

The changes in the peak output power of the seaplane under different propeller pitch angles are illustrated in Figure 11, with variations in thrust and torque shown in Figures 12 and 13, respectively. In the experiment conducted at an 11° pitch angle, the power output from the source was limited to 35 kilowatts, reaching the maximum rotational speed limit for the propeller of the RX1E-S electric seaplane. At this pitch angle, the propeller generates reduced thrust, necessitating a longer duration for completing a take-off task, leading to increased energy consumption. In the flight experiment at a 19° pitch angle, the propeller did not achieve its maximum rotational speed due to the limitation in power output, resulting in lower thrust for this flight task compared to the calculations in Section 2. Similarly, in the experiments at 13°, 15°, and 17° pitch angles, the thrust generated showed only minor differences due to the constraints of maximum rotational speed and power output. This is depicted in Figure 12, where the thrust curves are closely intertwined.

Additionally, we obtained power variation curves at different rotational speeds, as shown in Figure 14. We also monitored the efficiency of the motor and the controller, as illustrated in Figures 15 and 16. Both the motor and the controller exhibit a broad range of high efficiency, consistently achieving efficiency levels above 80%.

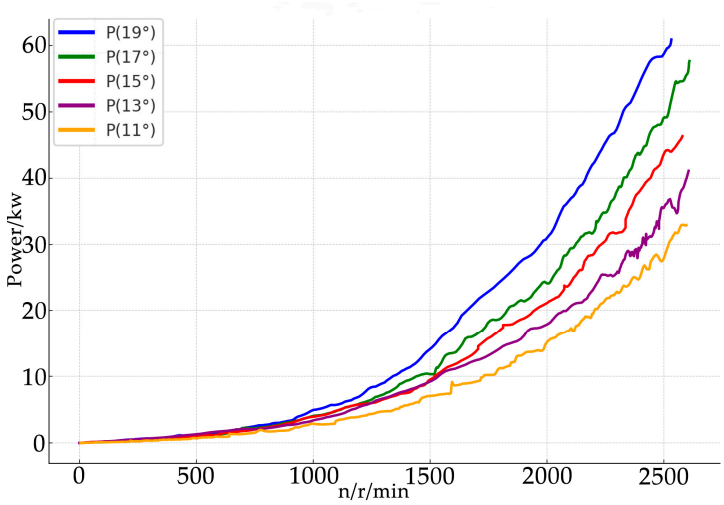

Figure 14. Power variation at different RPMs for the RX1E-S seaplane.

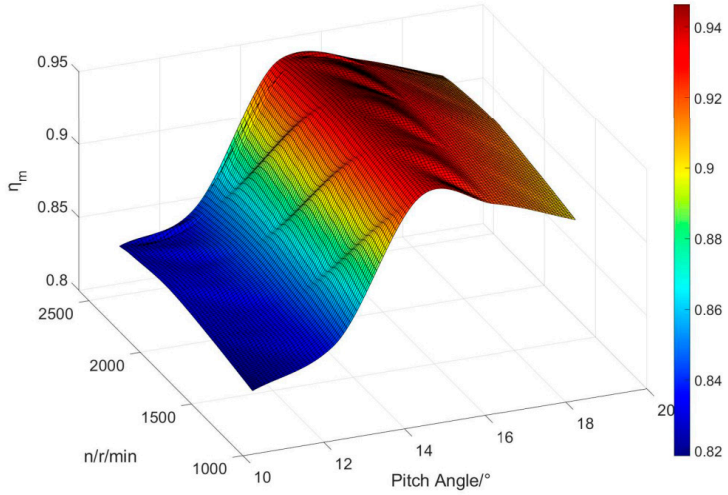

Figure 15. Motor efficiency under different conditions.

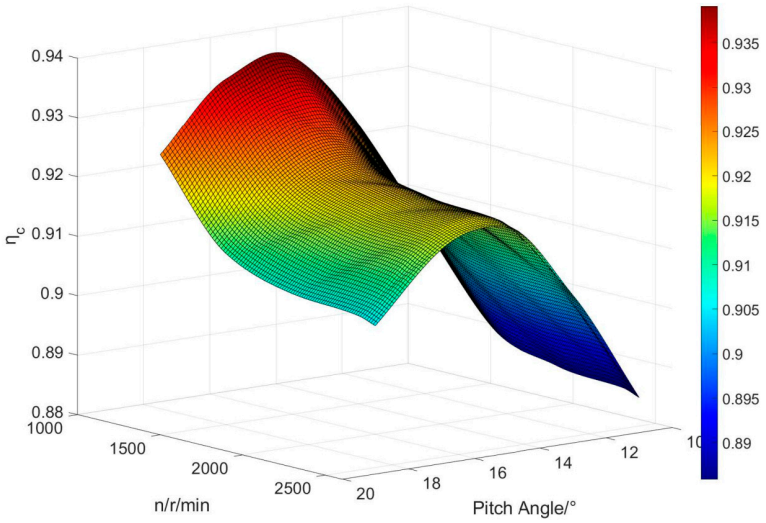

Figure 16. Controller efficiency under different conditions.

Finally, we conducted multiple repeated flight experiments for the same flight mission with five different propeller pitch angles. Based on the average values of each group, we

determined the total energy consumption for completing the flight mission at different pitch angles, as shown in Figure 17. The lowest energy consumption was observed at a pitch angle of 17°, amounting to 5.12 kWh, which is broadly in line with the results calculated earlier in the text, as shown in Figure 18. It was concluded that the optimal propeller pitch angle is around 17°, and the calculated energy consumptions are not significantly different. According to the calculations, using the optimal propeller pitch angle leads to a reduction of about 10.4% in energy consumption compared to the optimal pitch angle for the climbing phase, which is about 4.7% lower than the energy consumption at the optimal pitch angle for take-off taxiing.

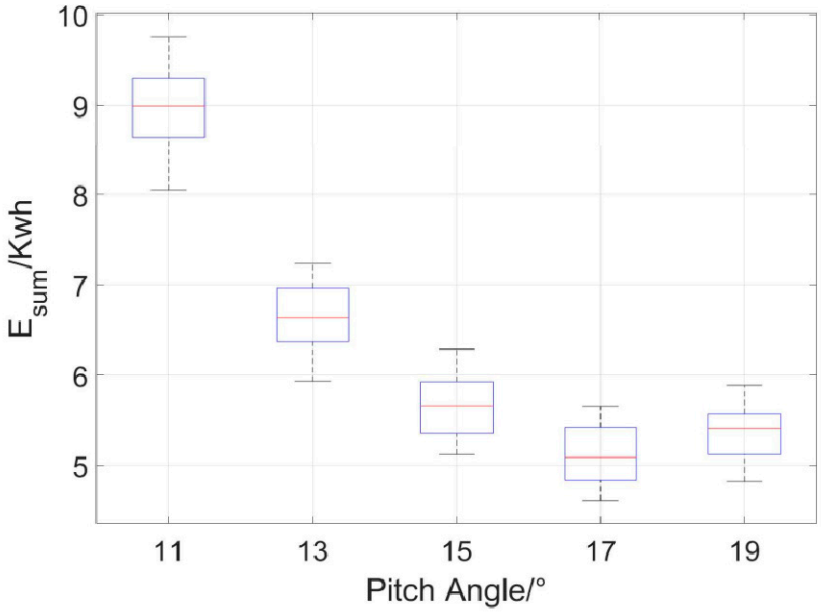

Figure 17. Energy consumption at different propeller pitch angles for the RX1E-S seaplane.

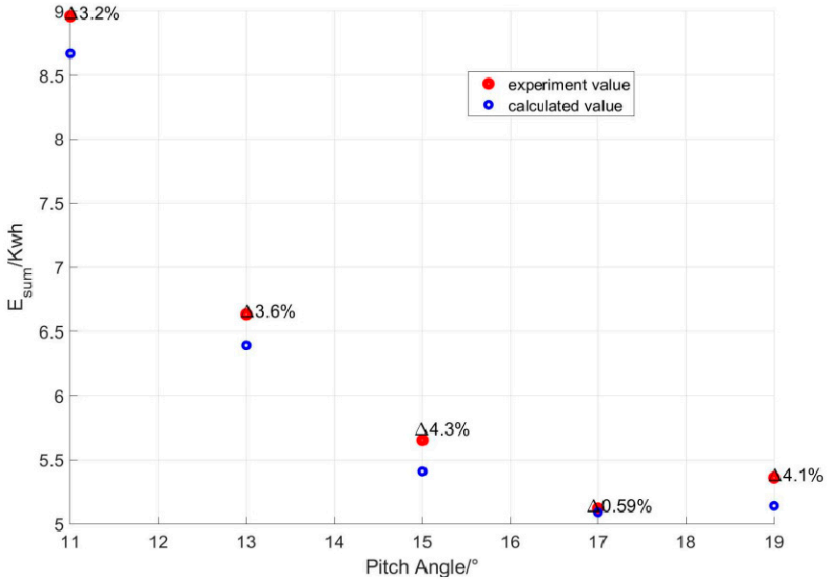

Figure 18. Comparison of experimental values and calculated values.

According to Figure 18, we can clearly observe discrepancy between the calculated values and the actual values. Our calculations are lower than the test values, which we attribute to the variance between the input parameters used in the model and the actual conditions. The tests were conducted outdoors, where external environmental factors

significantly influence the results. Despite incorporating numerous variable parameters to more accurately simulate the real environment, variations still exist due to rapidly changing meteorological conditions. Although there are some discrepancies, these do not affect the selection of the optimal propeller pitch angle. The calculated optimal pitch angle has been verified to still hold a significant advantage in experimental conditions.

Based on the prototype experiments, we confirmed the reliability and feasibility of the optimization method. This method can be applied to different electric seaplanes operating in their usual waters and carrying out common flight missions. By using the aforementioned method for numerical calculations, the optimal propeller pitch angle can be determined to minimize energy consumption. The optimization approach proposed in this paper explores and validates efficiency optimization for fixed-pitch propeller electric seaplanes, demonstrating the effectiveness and potential application value of this method.

In this experiment, we also identified several important issues. Higher propeller pitch angles provide the advantage of generating greater thrust, but they require a more powerful electrical system to support the increased power demand. This imposes a higher load on EPU, presenting challenges in optimizing the overall weight and heat dissipation of EPU. Through reasonable optimization of the EPU, determining important parameters like different power output levels for various types of electric seaplanes and selecting appropriate propeller pitch angles can bring valuable energy efficiency improvements. Using lower propeller pitch angles, although further reducing torque and slightly decreasing thrust, significantly lowers power consumption. Considering this characteristic, we can experiment with propellers having a higher-rated speed. However, it should be noted that lower pitch angles might result in insufficient thrust, requiring longer distances and times for takeoff, as well as extended climbing times to reach the predetermined cruising altitude in our seaplane experiments. In actual flying, small thrust can also lead to reduced feedback for the pilot operating the throttle lever.

These findings indicate that optimizing the design parameters of seaplanes can effectively reduce energy consumption during mission flights and enhance flight efficiency. This holds significant importance in advancing electric seaplane and green aviation technologies, providing substantial support and methodologies for the future sustainable development of the aviation field.

6. Conclusions

1. The overall efficiency of electric seaplanes is influenced by various external factors, among which the aquatic environment, meteorological characteristics, and flight missions significantly impact efficiency. By establishing mathematical models incorporating different parameters brought about by varying external environments, the seaplane's energy consumption can be calculated, thereby optimizing overall efficiency. The impact of flight missions is particularly significant. For two-seater electric seaplanes, which typically employ visual flight rules, the flight missions are relatively fixed. These types of seaplanes are generally used for pilot training, tourism, sightseeing, and short-distance flights. Frequent takeoffs, landings, climbs, and descents are required in water flying, making it valuable to optimize these stages.
2. Research indicates that the efficiency range of fixed-pitch propellers is limited, making it difficult to maintain optimal efficiency during different flight phases. Therefore, selecting the optimal propeller pitch angle to maintain the best efficiency during various operational phases of the seaplane can effectively improve the overall efficiency of the EPU, potentially reducing energy consumption by up to approximately 10.4%.
3. In practical tests, using the optimal propeller pitch angle has been shown to enhance propeller efficiency, thereby effectively reducing the duration of high power output from the motor and controller, and lowering the risk of EPU overheating.
4. This study proposes an optimization method for enhancing EPU efficiency based on propeller blade element theory. The efficiency and energy consumption of the propeller at different stages were calculated, identifying the points of highest effi-

ciency. These angles were then validated through experiments with an RX1E-S electric seaplane, proving the method's effectiveness and accuracy.

Author Contributions: Conceptualization, Z.L. and S.W.; methodology, Z.L.; validation, S.W., Z.L. and Q.Z.; formal analysis, S.W.; investigation, S.W.; resources, Q.Z.; data curation, Z.L.; writing—original draft preparation, Z.L.; writing—review and editing, Q.Z., S.W. and Z.L.; visualization, Q.Z.; supervision, Q.Z.; project administration, Q.Z. All authors have read and agreed to the published version of the manuscript.

Funding: This work was supported in part by the Natural Science Foundation of Liaoning Province through the Project under Grant 2022-KF-14-04, and in part by the Natural Science Foundation of Shenyang City through the Project under Grant 23-503-6-03.

Institutional Review Board Statement: Not applicable.

Informed Consent Statement: Not applicable.

Data Availability Statement: The raw data supporting the conclusions of this article will be made available by the authors on request.

Conflicts of Interest: The authors declare no conflict of interest.

References

1. Gitelman, L.; Kozhevnikov, M. Energy Transition Manifesto: A Contribution towards the Discourse on the Specifics Amid Energy Crisis. *Energies* **2022**, *15*, 9199. [CrossRef]
2. Zaporozhets, O.; Isaienko, V.; Synylo, K. Trends on current and forecasted aircraft hybrid electric architectures and their impact on environment. *Energy* **2020**, *211*, 118814. [CrossRef]
3. Donateo, T.; Spedicato, L. Fuel economy of hybrid electric flight. *Appl. Energy* **2017**, *206*, 723–738. [CrossRef]
4. Friedrich, C.; Robertson, P.A. Hybrid-electric propulsion for automotive and aviation applications. *CEAS Aeronaut. J.* **2015**, *6*, 279–290. [CrossRef]
5. Sahoo, S.; Zhao, X.; Kyprianidis, K. A Review of Concepts, Benefits, and Challenges for Future Electrical Propulsion-Based Aircraft. *Aerospace* **2020**, *7*, 44. [CrossRef]
6. Brelje, B.J.; Martins, J.R. Electric, hybrid, and turboelectric fixed-wing aircraft: A review of concepts, models, and design approaches. *Prog. Aerosp. Sci.* **2019**, *104*, 1–19. [CrossRef]
7. Salem, K.A.; Palaia, G.; Quarta, A.A. Review of hybrid-electric aircraft technologies and designs: Critical analysis and novel solutions. *Prog. Aerosp. Sci.* **2023**, *141*, 100924. [CrossRef]
8. Huang, J.; Yang, F.T. Development and challenges of new energy electric aircraft. *Acta Aeronaut. Astronaut. Sin.* **2016**, *37*, 57–68.
9. Ji, Z.; Rokni, M.M.; Qin, J.; Zhang, S.; Dong, P. Energy and configuration management strategy for battery/fuel cell/jet engine hybrid propulsion and power systems on aircraft. *Energy Convers. Manag.* **2020**, *225*, 113393. [CrossRef]
10. Yang, F.; Fan, Z.; Xiang, S.; Liu, Y.; Zhao, W. Technology innovation and Practice of electric aircraft in China. *Acta Aeronaut. Astronaut. Sin.* **2021**, *42*, 7–12.
11. Masri, J.; Dala, L.; Huard, B. A review of the analytical methods used for seaplanes' performance prediction. *Aircr. Eng. Aerosp. Technol.* **2019**, *91*, 820–833. [CrossRef]
12. Lei, T.; Min, Z.; Gao, Q.; Song, L.; Zhang, X.; Zhang, X. The architecture optimization and energy management technology of aircraft power systems: A review and future trends. *Energies* **2022**, *15*, 4109. [CrossRef]
13. Wang, S.; Zhang, Q.; Kang, G.; Fan, X.; Zhang, S.; Bao, J. An Optimization Method for Improving Efficiency of Electric Propulsion System of Electric Seaplane. *IEEE Access* **2023**, *11*, 31052–31061. [CrossRef]
14. Guo, F.; Li, C.; Liu, H.; Cheng, K.; Qin, J. Matching and performance analysis of a solid oxide fuel cell turbine-less hybrid electric propulsion system on aircraft. *Energy* **2023**, *263*, 125655. [CrossRef]
15. Uttekar, S.S.; Shendokar, Y.V.; Gupta, A.; Aparaj, P.; Karandikar, P.B. Power and Energy Density Analysis of Various Propulsion Systems. In *Global Emerging Innovation Summit (GEIS 2021)*; Bentham Science Publishers: Sharjah, United Arab Emirates, 2021; pp. 1–10.
16. Brophy, J.R. Perspectives on the success of electric propulsion. *J. Electr. Propuls.* **2022**, *1*, 9. [CrossRef]
17. Duan, X.; Sun, W.; Wei, M.; Zuo, Z.; Yang, Y. Investigation on the Hydrodynamics of Seaplane Takeoff Process. *Adv. Aeronaut. Eng.* **2019**, *10*, 94–101.
18. Wheeler, P.; Sirimanna, T.S.; Bozhko, S.; Haran, K.S. Electric/Hybrid-Electric Aircraft Propulsion Systems. *Proc. IEEE* **2021**, *109*, 1115–1127. [CrossRef]
19. Esteban, M.; Pérez-Carro, J.; Revuelta, A.; Mocholi, I. Power Management Strategies for Electric Aircraft Propulsion Systems: A Review. *Energies* **2019**, *12*, 3570. [CrossRef]
20. Xia, J.; Zhou, Z.; Xu, D.; Wang, Z. Aerodynamic and Propulsion Coupling Model of vector electric Propulsion System. *Acta Aeronaut. Astronaut. Sin.* **2023**, *44*, 135–147. (In Chinese) [CrossRef]

21. Wei, B.; Yang, Y.; Zhang, X.; Zhang, C. Energy efficiency optimization method for automatic pitch variable propeller electric propulsion System. *J. Aerosp. Power* **2023**, *38*, 717–727.
22. Shi, Z.; Wang, S.; Liu, W. Aircraft overall scheme optimization method based on improved particle swarm optimization. *J. Xi'an Aeronaut. Univ.* **2023**, *41*, 1–7.
23. Papadopoulos, K.I.; Nasoulis, C.P.; Ntouvelos, E.G.; Gkoutzamanis, V.G.; Kalfas, A.I. Power Flow Optimization for a Hybrid-Electric Propulsion System. *J. Eng. Gas Turbines Power* **2022**, *144*, 111013. [CrossRef]
24. Palaia, G.; Abu Salem, K. Mission Performance Analysis of Hybrid-Electric Regional Aircraft. *Aerospace* **2023**, *10*, 246. [CrossRef]
25. Benmoussa, A.; Gamboa, P.V. Effect of Control Parameters on Hybrid Electric Propulsion UAV Performance for Various Flight Conditions: Parametric Study. *Appl. Mech.* **2023**, *4*, 493–513. [CrossRef]
26. Hu, Q.; Wu, B.; Wang, M.Z.; Huang, M.; Jiang, R. Numerical Simulation of Wave Landing Loads Characteristics of Twin-Float Seaplane. *IOP Conf. Ser. Mater. Sci. Eng.* **2019**, *692*, 012024. [CrossRef]
27. Bai, L.; Chen, D.; Xiao, D.; Wang, J.; Zhou, G.; Xie, Y. Experimental and numerical analysis of underwater vehicle model based on Surface design for drag reduction. *J. Exp. Mech.* **2006**, *21*, 661–666.
28. Duan, X.; Sun, W.; Wei, M.; Yang, Y. Numerical simulation of amphibious aircraft taxiing at high speed on water using OpenFoam. *Acta Aeronaut. Astronaut. Sin.* **2019**, *40*, 522330.
29. Zhao, L.J.; Tian, M.W.; Li, J.K.; Wang, M.; Liu, D. Float Design and Takeoff Taxiing of Electric Seaplanes. *Acta Aeronaut. Astronaut. Sin.* **2021**, *42*, 41–52.
30. Sun, J.J.; Ma, D.L. Estimation of Resistance During High-Speed Static Water Taxiing of Hull-Type Seaplanes. *J. Beijing Univ. Aeronaut. Astronaut.* **2015**, *41*, 925–929. [CrossRef]
31. Wu, J.; Gao, F.; Huang, M.; Tong, S.X.; Yang, F.T. Simulation and Analysis of the Static Water Takeoff Resistance Peak for a Certain Type of Electric Seaplane. *Flight Dyn.* **2022**, *4*, 81–86.
32. Zhou, K.; Shang, D.; Lin, Y.; Zhang, J. Simulation and energy efficiency optimization method of electric propulsion ship. *China Navig.* **2022**, *45*, 123–128.